Proceedings of the 9th International Conference on Structural Dynamics, EURODYN 2014
Porto, Portugal, 30 June - 2 July 2014
A. Cunha, E. Caetano, P. Ribeiro, G. Müller (eds.)
ISSN: 2311-9020; ISBN: 978-972-752-165-4

A rotating ring in contact with a stationary load as a model for a flexible train wheel

T. Lu, A.V. Metrikine
Faculty of Civil Engineering and Geosciences, Delft University of Technology, Stevinweg 1, 2628 CN Delft, The Netherlands
email: T.Lu-2@tudelft.nl, A.Metrikine@tudelft.nl

ABSTRACT: A load moving on a center-fixed ring and the reciprocal problem, namely a rotating ring subjected to a moving load have been used in several works to study the tire dynamics. In contrast, very few papers exist in which the ring model has been used in order to study the dynamics of a train wheel. In this paper, a thin ring model is introduced to model a flexible train wheel with distributed springs acting in the radial, circumferential and rotational directions to study the wheel dynamic response. A so-called "method of images" is applied to solve the governing equations. The idea of this method is that the response of the rotating ring to a stationary load is equivalent to the response of an axially moving, infinitely long beam subjected to a set of loads located equidistantly on the beam. Taking advantage of linearity of the problem, the response is obtained as a superposition of the responses to the individual loads. The method of images combined with the contour integration technique, allows to obtain an exact analytical solution to the problem that includes neither infinite series nor integrals. The exact maximum bending moment in the ring obtained using the method of images is compared to that resulting from a series representation of the solution based on the modal expansion. The results show that many terms in the modal expansion are necessary in order to accurately approximate the exact solution. This means that the method of images is significantly more efficient than the modal expansion method.

KEY WORDS: Flexible train wheel; Rotating ring; Method of the images.

1 INTRODUCTION

The vibrations of rotating rings were studied by many authors. The influence of different factors, such as shear deformation, rotatory inertia, non-linear behavior etc., was considered in the literature. The main engineering application of those studies was in the field of dynamics of the pneumatic tires. Based on thin shell/ring theory, Soedel [1] studied the dynamic response of rolling tires by formulating the three-dimensional Green's function based on the natural modes and frequencies derived from the non-rotating tire. The contact force was assumed to travel around the tire. Padovan [2] investigated the effect of internal damping on the development of standing waves with the help of the classical ring on elastic foundation model. Endo [3] derived the equations of motion from the Hamilton's principle and included the initial tension due to rotation. Experiments were conducted by Endo to verify the model and comparisons were made between the model he used and some models in the literature. Huang and Soedel analyzed the free and forced vibrations of rotating thin rings and shells on elastic foundation in Ref. [4]. A modal expansion was implemented based on so-called "rotating modes". The resonant conditions of a rotating cylindrical shell were obtained for four cases by Huang and Hsu in [5]. Kim and Bolton [7] illustrated the effect of rotation by assuming a wave-like solution. They concluded that the dispersion curves in the rotating and fixed coordinate systems can be correlated kinematically.

In this paper, a thin ring model with distributed springs resisting in the radial, circumferential and rotational directions is introduced to describe the dynamics of a flexible train wheel. This springs represent the reaction of spokes that would connect the hub and the rim of the wheel. A so-called "method of the images" [6] is applied to solve the problem. The idea of this method is that the response of a finite length system to a load is equivalent to the response of a part of an infinity long system described by the same equations and subjected to an infinite set of equally-spaced loads. The maximum change of curvature which represents the maximum bending moment of the ring using the modal analysis technique is compared with the exact result obtained by the method of the images. The comparison shows that the latter method is superior to the commonly used modal analysis.

2 MODEL AND EQUATIONS OF MOTION

2.1 *Model*

The model of a flexible train wheel is shown in Figure 1 along with the coordinate system. The hub and the rim are connected by visco-elastic spokes which are modeled as distributed springs.

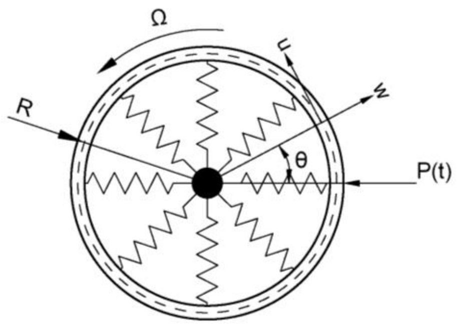

Figure 1. Rotating ring under a stationary load.

It is assumed that the mean radius of the wheel is R and w and u are the small displacements in the radial and circumferential directions, respectively. The stiffnesses of the radial, circumferential and rotational springs per unit length are designated as k_r , k_c and k_{rot} respectively. It is also assumed that all springs possess viscosity per unit length equal to σ . Furthermore, ρ is the mass density of the rim, E is the Young's modulus, F is the cross-sectional area and I is the cross sectional moment of inertia. $P(t)=P_0\exp(\mathrm{i}\tilde{\Omega}_f t)$ is the magnitude of the radial point load which represents the contact force between the rail and the wheel. Ω is the angular frequency of the wheel rotation.

The stiffness of the rotational spring can be related to that of the circumferential one by considering the spoke as an Euler-Bernoulli beam clamped at the hub. Under this assumption, the rotational stiffness can be expressed in terms of the circumferential stiffness k_c as

$$k_{rot}=\frac{R^2}{3}k_c\,. \tag{1}$$

2.2 *Equations of motion*

The derivation of the equations of motion can be done similarly to Ref. [4] with the help of the Hamilton's principle. Since the rotational springs are introduced, the potential energy stored by the rotational springs should also be included. So the total potential energy stored by all the springs is

$$U=\int_0^{2\pi}\frac{1}{2}\left(k_c u^2+k_r w^2+k_{rot}\beta^2\right)Rd\theta \tag{2}$$

where $\beta=\left(\partial w/\partial\theta-u\right)/R$ is the rotation angle.

Then, following the procedure outlined in Ref. [4], the equations of motion for the ring in the rotating with the ring reference system can be obtained in the following form:

$$\frac{EI}{R^4}\left(\partial_{\theta\theta\theta}w-\partial_{\theta\theta}u\right)-\frac{EF}{R^2}\left(\partial_\theta w+\partial_{\theta\theta}u\right)-\rho F\Omega^2\left(2\partial_\theta w+\partial_{\theta\theta}u\right)$$
$$+\sigma\partial_t u+\rho F\left(\partial_{tt}u+2\Omega\partial_t w\right)+k_c u+\frac{k_c}{3}\left(u-\partial_\theta w\right)=0,$$
$$\frac{EI}{R^4}\left(\partial_{\theta\theta\theta\theta}w-\partial_{\theta\theta\theta}u\right)+\frac{EF}{R^2}\left(w+\partial_\theta u\right)+\rho F\Omega^2\left(2\partial_\theta u-\partial_{\theta\theta}w\right)+\sigma\partial_t u$$
$$+\rho F\left(\partial_{tt}w-2\Omega\partial_t u\right)+k_r w+\frac{k_c}{3}\left(\partial_\theta u-\partial_{\theta\theta}w\right)=-\frac{P(t)}{R}\delta\left(\theta+\Omega t\right). \tag{3}$$

In equations (3), ∂_θ designates the partial derivative with respect to θ while ∂_t represents the partial derivative with respect to time. The displacements should also satisfy the periodicity condition:

$$\begin{aligned}u(\theta+2\pi)&=u(\theta),\\ w(\theta+2\pi)&=w(\theta).\end{aligned} \tag{4}$$

Equations (3) can be analyzed by means of the commonly used modal analysis, see Ref. [4], for example. In this paper, however, a more efficient method of the images will be employed as described in the next Section.

3 SOLUTIONS ACCORDING TO THE METHOD OF THE IMAGES

3.1 *Description of " method of images"*

The method of the images has been first applied to study the steady-state response of an elastic ring subjected to a moving load in [6]. The idea of this method is that the response of a bounded (in our case ring-like) system to a single load is equivalent to the response of a part of an infinity long system (described by the same equations) subjected to an infinite set of loads. In other words, the method utilizes the fact that by introducing additional loads one can satisfy the boundary conditions. These loads are called images since their locations are normally mirrored to the real load with respect to the boundaries. In the considered case, to satisfy the periodicity of the displacements, one should introduce infinitely many equivalent loads at fixed distance $2\pi R$ from each other, see Figure 2.

Since the problem is linear, the ring response is a sum of the response of the "extended ring" to all the individual loads.

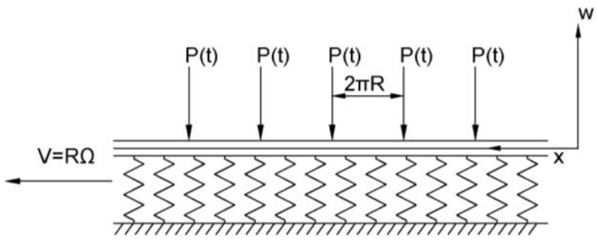

Figure 2. Illustration of the "method of images".

The ring is extended to an infinitely long straight "beam", it is more convenient to use the translational coordinate $x=R\theta$. Substituting $\Omega=v/R$ and re-arranging all the terms, the equations of motion (3) can be re-written as

$$\rho F\partial_{tt}u+\sigma\partial_t u-E\left(F+\frac{I}{R^2}\right)\partial_{xx}u+\frac{E}{R}(I\partial_{xxx}w-F\partial_x w)$$
$$+\frac{2v\rho F}{R}\partial_t w-\rho Fv^2\left(\frac{2}{R}\partial_x w+\partial_{xx}u\right)+\frac{k_c}{3}\left(u-R\partial_x w\right)=0,$$

$$\rho F\partial_{tt}w+\partial_t w+EI\partial_{xxxx}w+(k_r+\frac{EF}{R})w-\frac{E}{R}\left(I\partial_{xxx}u-F\partial_x u\right)$$
$$-\frac{2v\rho F}{R}\partial_t u+\rho Fv^2(\frac{2}{R}\partial_x u-\partial_{xx}w)+\frac{k_c R}{3}\left(\partial_x u-R\partial_{xx}w\right)$$
$$=-P\left(t\right)\sum_{n=-\infty}^{+\infty}\delta\left(x+vt+2n\pi R\right). \tag{5}$$

It is customary to study the response in a reference system moving together with the loads. Introducing the new reference system according to $\{\xi=x+vt,\,t=t\}$, the equations of motion can be transformed to

$$\rho F\partial_{tt}u+\sigma(\partial_t u+v\partial_\xi u)-E(F+\frac{I}{R^2})\partial_{\xi\xi}u+\frac{E}{R}(I\partial_{\xi\xi\xi}w-F\partial_\xi w)$$
$$+\frac{2v\rho F}{R}\partial_t w+2v\rho F\partial_{\xi t}u+\frac{k_c}{3}(u-R\partial_\xi w)=0,$$

$$\rho F\partial_{tt}w+\sigma(\partial_t w+v\partial_\xi w)+EI\partial_{\xi\xi\xi\xi}w+(k_r+\frac{EF}{R})w-$$
$$\frac{E}{R}(I\partial_{\xi\xi\xi}u-F\partial_\xi u)-\frac{2v\rho F}{R}\partial_t u+2v\rho F\partial_{\xi t}w+$$
$$\frac{k_c R}{3}(\partial_\xi u-R\partial_{\xi\xi}w)=-P(t)\sum_{n=-\infty}^{+\infty}\delta(\xi+2n\pi R). \tag{6}$$

Since the exact solution is the summation of the responses to all the individual loads and all the loads generate equivalent but shifted with respect to each other displacement fields, it is actually sufficient to obtain the response of the axially moving “extended ring” to a single load and then sum up this response infinitely many times accounting for the spatial shift $2\pi R$. One of the main advantages of the method of the images is that the aforementioned infinite summation can be computed analytically, using the formulae for an infinite geometric progression.

To proceed, the following dimensionless variables and parameters are introduced:

$$\begin{aligned}&\alpha=\sqrt{EI/\rho F},\ h=\sqrt{k_r/(\rho F)},\\&\tau=ht,\ y=\xi\sqrt{h/\alpha},V=v/\sqrt{2\alpha h},\\&A=\sqrt{E/\rho}/(hR),B=\sqrt{E/(\rho\alpha h)},\\&\varepsilon=\sigma/(\rho Fh),K=k_c/k_r,\\&P_0=P/\sqrt{\rho F\alpha h},\ \Omega_f=\tilde{\Omega}_f/h.\end{aligned} \tag{7}$$

Employing the above dimensionless variables and parameters and considering a single load $n=0$, Equations (6) can be written as

$$\partial_{\tau\tau}u_s+\varepsilon(\partial_\tau u_s+\sqrt{2}V\partial_y u_s)-(B^2+\frac{A^2}{B^2})\partial_{yy}u_s+\frac{A}{B}\partial_{yyy}w_s$$
$$-AB\partial_y w_s+\frac{2\sqrt{2}VA}{B}\partial_\tau w_s+2\sqrt{2}V\partial_{y\tau}u_s+\frac{4K}{3}u_s-\frac{KB}{3A}\partial_y w_s=0,$$

$$\partial_{\tau\tau}w_s+\varepsilon(\partial_\tau w_s+\sqrt{2}V\partial_y w_s)+\partial_{yyyy}w_s+(1+A^2)w_s-$$
$$\frac{A}{B}\partial_{yyy}u_s-AB\partial_y u_s-\frac{2\sqrt{2}VA}{B}\partial_\tau u_s+2\sqrt{2}V\partial_{y\tau}w_s+$$
$$\frac{KB}{3A}\partial_y u_s-\frac{KB^2}{3A^2}\partial_{yy}w_s=-P_0\sqrt{\alpha/h}\exp(i\Omega_f\tau)\delta(y),$$
$$-\infty<y<+\infty,\ -\infty<\tau<+\infty. \tag{8}$$

The governing equations (8) can be solved by means of application of the integral Fourier transform. Defining this transform as

$$\begin{bmatrix}\tilde{\tilde{w}}_{\omega,k}\\\tilde{\tilde{u}}_{\omega,k}\end{bmatrix}=\int_{-\infty}^{+\infty}\int_{-\infty}^{+\infty}\begin{bmatrix}w^s\\u^s\end{bmatrix}\exp(iky-i\omega\tau)d\tau dy \tag{9}$$
$$\left\{\tilde{\tilde{w}}_{\omega,k};\tilde{\tilde{u}}_{\omega,k}\right\}=\int_{-\infty}^{+\infty}\int_{-\infty}^{+\infty}\left\{w^s;u^s\right\}\exp(iky-i\omega\tau)d\tau dy$$

and applying it to Eq.(8), one obtains

$$\begin{aligned}&\tilde{\tilde{w}}_{\omega,k}\Delta_{w1}+\tilde{\tilde{u}}_{\omega,k}\Delta_{u1}=-2\pi P_0\sqrt{\alpha/h}\delta(\omega-\Omega_f),\\&\tilde{\tilde{w}}_{\omega,k}\Delta_{w2}+\tilde{\tilde{u}}_{\omega,k}\Delta_{u2}=0,\end{aligned} \tag{10}$$

where

$$\Delta_{u1}=\frac{-3iA^3B^2k-6i\sqrt{2}A^3V\omega-iKB^2Ak-3iA^3k^3}{3BA^2},$$

$$\Delta_{w1}=(-3\omega^2BA^2+6\sqrt{2}VBA^2\omega k+3i\varepsilon BA^2\omega-$$
$$3i\varepsilon BA^2\sqrt{2}Vk+3BA^2k^4+3BA^2+3BA^4+KB^3k)/3BA^2, \tag{11}$$

$$\Delta_{u2}=-(-3B^2A\omega^2+6\sqrt{2}VB^2A\omega k+3i\varepsilon B^2A\omega-$$
$$3i\varepsilon B^2A\sqrt{2}Vk+4KB^2A+3AB^4k^2+3A^3k^2)/3B^2A,$$

$$\Delta_{w2}=\frac{3iA^2B^3k+6i\sqrt{2}A^2BV\omega+iKB^3k+3iA^2Bk^3}{3AB^2}.$$

Solving equation (10) for the Fourier displacements $\tilde{\tilde{w}}_{\omega,k}$ and $\tilde{\tilde{u}}_{\omega,k}$ one obtains

$$\begin{aligned}&\tilde{\tilde{w}}_{\omega,k}=2\pi P_0\sqrt{\alpha/h}\Delta_{u2}/\Delta,\\&\tilde{\tilde{u}}_{\omega,k}=2\pi P_0\sqrt{\alpha/h}\Delta_{w2}/\Delta,\end{aligned} \tag{12}$$

where

$$\Delta(\omega,k)=\Delta_{w1}\Delta_{u2}-\Delta_{w2}\Delta_{u1}. \tag{13}$$

The next step is to invert the obtained solutions to the time domain by using the inverse Fourier transform. This can be done by following the procedure introduced in Ref. [6]. After obtaining the solutions in the time domain for the single load case, the exact solution can be found by summarizing it infinitely many times with the space shift $2n\pi R$. After some manipulations, the analytical expressions of the displacements of the ring can be derived as

for $-2\pi R\sqrt{h/\alpha}\le\xi\le 0$:

$$\begin{bmatrix}u\\w\end{bmatrix}=\frac{iP_0}{a_7}\sqrt{\frac{\alpha}{h}}\left(\sum_m\begin{bmatrix}B_u^m\\B_w^m\end{bmatrix}\frac{\exp(-ik_m\xi)}{1-\exp(i2\pi Rk_m\sqrt{h/\alpha})}\right.$$
$$\left.-\sum_n\begin{bmatrix}B_u^n\\B_w^n\end{bmatrix}\frac{\exp(-ik_n(\xi+2\pi R\sqrt{h/\alpha}))}{1-\exp(i2\pi Rk_n\sqrt{h/\alpha})}\right)\exp(i\Omega_f\tau), \tag{14}$$

for $0<\xi<2\pi R\sqrt{h/\alpha}$:

$$\begin{bmatrix} u \\ w \end{bmatrix} = \frac{\mathrm{i}P_0}{a_7}\sqrt{\frac{\alpha}{h}}\left(\sum_m \begin{bmatrix} B_u^m \\ B_w^m \end{bmatrix} \frac{\exp(-\mathrm{i}k_m(\xi - 2\pi R\sqrt{h/\alpha}))}{1-\exp(i2\pi Rk_m\sqrt{h/\alpha})}\right.$$
$$\left. -\sum_n \begin{bmatrix} B_u^n \\ B_w^n \end{bmatrix} \frac{\exp(-ik_n\xi)}{1-\exp(-i2\pi Rk_n\sqrt{h/\alpha})}\right)\exp(\mathrm{i}\Omega_f\tau), \tag{15}$$

where

$$\begin{bmatrix} B_u^m \\ B_w^m \end{bmatrix} = \begin{bmatrix} \Delta_{w2}(\Omega_f, k_m) \\ \Delta_{u2}(\Omega_f, k_m) \end{bmatrix} \frac{(k-k_m)}{\prod_{l=1}^{6}(k-k_l)},$$
$$\begin{bmatrix} B_u^n \\ B_w^n \end{bmatrix} = \begin{bmatrix} \Delta_{w2}(\Omega_f, k_n) \\ \Delta_{u2}(\Omega_f, k_n) \end{bmatrix} \frac{(k-k_n)}{\prod_{l=1}^{6}(k-k_l)}, \tag{16}$$

$a_7 = B^2$ and k_n and k_m are the complex roots of the equation $\Delta(\Omega_f, k) = 0$ located in the lower and upper half-planes of the complex k-plane, respectively. The real part of the above-given solution should be taken if the time signature of the load is given as $P(t) = P_0\cos(\tilde{\Omega}_f t)$, whereas the imaginary part corresponds to $P(t) = P_0\sin(\tilde{\Omega}_f t)$.

To visualize the obtained solution the shape of the ring is shown in Figure 3 for the following parameters of the model, which are the same as in Ref. [6]:

$$\begin{aligned} &E = 2.06\times10^{11}\,N/m^2, \quad \rho = 7800kg/m^3, \\ &F = 1.5\times10^{-3}m^2, \ I = 2.83\times10^{-6}m^4, \\ &R = 0.3m, k_r = 6\times10^7\,N/m^2, \\ &k_c = 1.8\times10^7\,N/m^2 \\ &P_0 = 50KN, \sigma = 2\times10^4\,Ns/m^2, \\ &v = R\Omega = 100m/s \end{aligned} \tag{17}$$

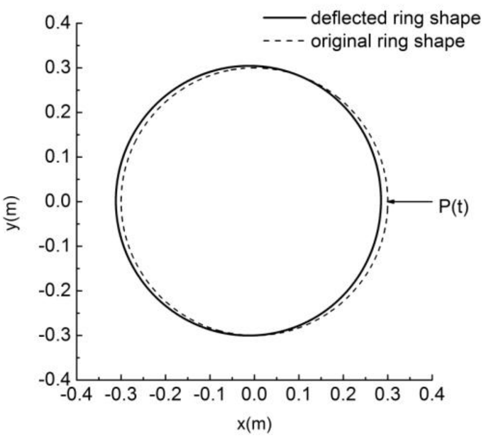

Figure 3. The ring shape for $v = 100m/s$.

Figure 3 clearly shows that the solution obtained by the method of the images satisfies the periodicity condition, Eq. (4) for the constant load($\Omega_f = 0$). For harmonically time varying load, the same conclusion holds.

In the next Section the obtained solution is applied for the assessment of the bending moment in the contact point and, based on this assessment, the efficiency of the presented herein method is elucidates relative to the commonly adopted modal analysis.

3.2 *Comparison of the efficiency of the method of the images and modal analysis*

The moment in the contact area between the spokes and the wheel rim is of importance because is a “hot spot” that governs the wheel fatigue. In this section, the maximum value of this moment is computed using both the modal analysis and the method of the images. The latter method allows to obtain an exact expression for the moment, this expression containing a summation of six terms only. On the contrary, the modal analysis results in a solution in the form of an infinite series which, as shown below, converges quite poorly to the exact value of the moment.

The maximum change of curvature can equivalently represent the maximum bending moment because $M = EIK_\theta$. The expression of the change of curvature K_θ reads

$$K_\theta = \frac{\partial_\theta u - \partial_{\theta\theta} w}{R^2} = \frac{1}{R}\partial_x u - \partial_{xx} w = \frac{\sqrt{h/\alpha}}{R}\partial_\xi u - \frac{h}{\alpha}\partial_{\xi\xi} w \tag{18}$$

Expression for $\partial_\xi u$ and $\partial_{\xi\xi} w$ can be obtained directly by differentiating equations (14) and (15)
for $-2\pi R\sqrt{h/\alpha} \le \xi \le 0$:

$$\partial_\xi u = \frac{iP_0\sqrt{\alpha/h}}{a_7}\exp(i\Omega_f\tau)\{ \sum_m B_u^m \frac{\exp(-ik_m\xi)}{1-\exp(i2\pi Rk_m\sqrt{h/\alpha})}(ik_m) - \sum_n B_u^n \frac{\exp(-ik_n(\xi + 2\pi R\sqrt{h/\alpha}))}{1-\exp(i2\pi Rk_n\sqrt{h/\alpha})}(-ik_n)\},$$
$$\partial_{\xi\xi} w = \frac{iP_0\sqrt{\alpha/h}}{a_7}\exp(i\Omega_f\tau)\{ \sum_m B_w^m \frac{\exp(-ik_m\xi)}{1-\exp(i2\pi Rk_m\sqrt{h/\alpha})}(-k_m^2) - \sum_n B_w^n \frac{\exp(-ik_n(\xi + 2\pi R\sqrt{h/\alpha}))}{1-\exp(i2\pi Rk_n\sqrt{h/\alpha})}(-k_n^2)\}, \tag{19}$$

for $0 < \xi < 2\pi R\sqrt{h/\alpha}$:

$$\partial_\xi u = \frac{iP_0\sqrt{\alpha/h}}{a_7}\exp(i\Omega_f\tau)\{$$
$$\sum_m B_u^m \frac{\exp(-ik_m(\xi-2\pi R\sqrt{h/\alpha}))}{1-\exp(i2\pi Rk_m\sqrt{h/\alpha})}(-ik_m)$$
$$-\sum_n B_u^n \frac{\exp(-ik_n\xi)}{1-\exp(-i2\pi Rk_n\sqrt{h/\alpha})}(-ik_n)\}, \tag{20}$$
$$\partial_{\xi\xi} w = \frac{iP_0\sqrt{\alpha/h}}{a_7}\exp(i\Omega_f\tau)\{$$
$$\sum_m B_w^m \frac{\exp(-ik_m(\xi-2\pi R\sqrt{h/\alpha}))}{1-\exp(i2\pi Rk_m\sqrt{h/\alpha})}(-k_m^2)$$
$$-\sum_n B_w^n \frac{\exp(-ik_n\xi)}{1-\exp(-i2\pi Rk_n\sqrt{h/\alpha})}(-k_n^2)\}.$$

Using the above-given equations, the maximum change of curvature can be calculated. In order to get the maximum change of curvature by modal analysis, the modal expansion method proposed in Ref. [4] is implemented.

The results are shown in Figure 4, which is plotted using the parameters values given by Eq. (17) and $\Omega_f = 0$ (constant load).

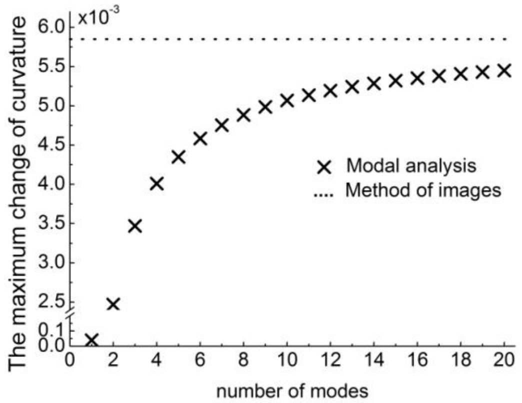

Figure 4. The convergence of modal analysis.

The horizontal dotted line in Figure 4 represents the exact solution for the maximum change of curvature obtained using the method of the images. For the modal analysis, the number of modes considered here is 20. The plot clearly shows that in order to predict the maximum change of curvature accurately, by means of the modal analysis a large number of modes should be accounted for and rather erroneous results could be obtained with a usually adopted 10-20 modes approximation.

4 CONCLUSIONS

A model of a rotating ring under a stationary radial load has been introduced in this paper with the aim to predict the dynamics of a flexible train wheel as would be observed in a laboratory testing with a fixed axis. The wheel is assumed to consist of a flexible rim attached to the hub by spokes, whose visco-elastic reactions in the radial, circumferential and rotational directions are accounted for in the model.

Along with the introduction of the new model of a flexible train wheel, the original result of this paper consists in the application of the method of the images for the analysis of the ring deflections and curvature. It has been shown that this method allows to obtain an exact analytical expression for the ring response. It has also been suggested that the method of the images is superior to the commonly adopted modal analysis as the latter would predict non-conservative values for the bending moment in the ring unless a large number of the modes would be accounted for.

REFERENCES

[1] W. Soedel, On the dynamic response of rolling tires according to thin shell approximations, *Journal of Sound and Vibration* 41 (2) (1975) 233-246.
[2] J. Padovan. On viscoelasticity and standing waves in tires, *Tire Science and Technology* 4 (4) (1976) 233-246.
[3] M. Endo, K. Hatamura, M. Sakata, O. Taniguchi, Flexural vibration of a thin rotating ring, *Journal of Sound and Vibration* 92 (2) (1984) 261-272.
[4] S.C. Huang, W. Soedel, Effects of coriolis acceleration on the free and forced in-plane vibrations of rotating rings on elastic foundation, *Journal of Sound and Vibration* 115 (2) (1987) 253-274.
[5] S.C. Huang, B.S. Hsu, Resonant phenomena of a rotating cylindrical shell subjected to a harmonic moving load, *Journal of Sound and Vibration* 136 (2) (1990) 215-228.
[6] A.V. Metrikine, M.V. Tochilin, Steady-state vibrations of an elastic ring under a moving load, *Journal of Sound and Vibration* 232 (3) (2000) 511-524.
[7] Y.J. Kim, J.S. Bolton, Effects of rotating on the dynamics of a circular cylindrical shell with applications to tire vibration, *Journal of Sound and Vibration* 275 (3) (2004) 605-621.